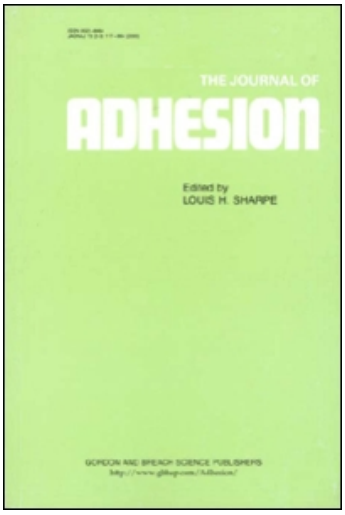

The Journal of Adhesion
Publication details, including instructions for authors and subscription information:
http://www.informaworld.com/smpp/title~content=t713453635

Development of a Computer Program for the Design of Adhesive Joints

Lucas F. M. da Silva[a]; Ricardo F. T. Lima[a]; R. M. S. Teixeira[a]
[a] Department of Mechanical Engineering, Faculty of Engineering, University of Porto, Porto, Portugal

Online publication date: 19 November 2009

To cite this Article da Silva, Lucas F. M. , Lima, Ricardo F. T. and Teixeira, R. M. S.(2009) 'Development of a Computer Program for the Design of Adhesive Joints', The Journal of Adhesion, 85: 12, 889 — 918
To link to this Article: DOI: 10.1080/00218460903307761
URL: http://dx.doi.org/10.1080/00218460903307761

The Journal of Adhesion, 85:889–918, 2009

ISSN: 0021-8464 print/1545-5823 online
DOI: 10.1080/00218460903307761

Taylor & Francis
Taylor & Francis Group

Development of a Computer Program for the Design of Adhesive Joints

Lucas F. M. da Silva, Ricardo F. T. Lima, and R. M. S. Teixeira
Department of Mechanical Engineering, Faculty of Engineering, University of Porto, Porto, Portugal

Adhesive joints are increasingly being used due to their improved mechanical performance and a better understanding of the mechanics of failure. To predict the joint strength, one must have the stress distribution and a suitable failure criterion. The literature contains many closed-form solutions for the stress distribution. However, the models are sometimes difficult to implement and use. The objective of the present work was to compile existing models of increasing complexity into user friendly software. Three main situations were considered: elastic adherends and adhesive, elastic adherends with nonlinear adhesive and nonlinear analyses for both adherends and adhesive. The adherends were both isotropic (metals) and anisotropic (composites). The joints considered are the single and double lap joints for most of the models. However, a sandwich model initially proposed by Crocombe can be used for any type of joint provided the boundary conditions are known. For each model proposed the compatible failure criteria are included to enable the user not only to have the stress distribution but also the failure load for a given joint/load scenario. Experimental tests corresponding to the three cases described above were carried out to validate the models implemented.

Keywords: Adhesive joints; Closed-form models; Design; Software

1. INTRODUCTION

There are many analytical models in the literature for obtaining stress and strain distributions. Many closed-form models are based on modified shear-lag equations, as proposed originally by Volkersen [1]. Aside from the shear-lag analysis technique, other workers have

Received 7 February 2009; in final form 2 June 2009.
Address correspondence to Lucas F. M. da Silva, Departamento de Engenharia Mecânica, Faculdade de Engenharia, Universidade do Porto, Rua Dr. Roberto Frias, Porto 4200-465, Portugal. E-mail: lucas@fe.up.pt

TABLE 1 Software Packages Available in the Market (adapted from [9]).

Name	Supplier	Application	Features
BOLT	G.S. Springer, Stanford University	Design of pin-loaded holes in composites	• Prediction of failure strength and failure mode • Three types of bolted joints: Joints with a single hole, Joints with two identical holes in a row, Joints with two identical holes in tandem • Applicable to uniform tensile loads and symmetric laminates
BISEPSLOCO	AEA Technology, UK	Closed form computer code for predicting stresses and strains in adhesively bonded single-lap joints	• Tensile/shear/bending moment loading • Adhesive peel and shear stress predictions • Allowance for plasticity in adhesive layer • Thermal stress analysis
BISEPSTUG	AEA Technology, UK	Closed form computer code for predicting stresses and strains in adhesively bonded coaxial joints	• Stepped and profiled joints • Orthotropic adherends • Torsional and axial loading • Allowance for plasticity in adhesive layer • Thermal stress analysis
CoDA	National Physical Laboratory, UK	Preliminary design of composite beams and panels, and bolted joints	• Synthesis of composite material properties (lamina and laminates for a range of fibre formats) • Parametric analyses • Panel and beam design • Bonded and bolted double shear joints • Bearing, shear-out, pin shear, and by-pass tensile failure prediction
DLR	DLR Mitteilung, Germany	Preliminary design of composite joints	• Adhesively bonded and bolted joints • Linear-elastic and linear-elastic/plastic behavior • Tension and shear loading • Symmetric and asymmetric lap joints • Bearing, shear-out, pin shear and by-pass tensile failure prediction (washers and bolt tightening)

FELOCO	AEA Technology, UK	Finite element module computer code for predicting stresses and strains in adhesively bonded lap shear joints	• Stepped and profiled joints • Tensile/shear/bending moment/pressure loading • Linear and non-linear analysis • Peel, shear, and longitudinal stress predictions in adhesive layer and adherends • Thermal stress analysis for adherend and adhesive joined systems include: Lap and butt joints, Sandwich structures, Bushes/gears/bearings/ shafts/pipes/threaded fittings • Elastic analysis • Creep/fatigue effects on joint stiffness (graphical)
PAL	Permabond, UK	"Expert" system for adhesive selection	• Joint strength • Correction factors (temperature and fatigue)
RETCALC	Loctite, UK	Interactive windows based software general purpose	• ESDU 78042 Shear stresses in the adhesives in bonded joints. Single-step double-lap joints loaded in tension • ESDU 79016 Inelastic shear stresses and strains in the adhesives bonding lap joints loaded in tension or shear (computer program) • ESDU 80011 Elastic stresses in the adhesive in single step double-lap bonded joints • ESDU 80039 Elastic adhesive stresses in multi-step lap joints loaded in tension (computer program) • ESDU 81022 Guide to the use of data items in the design of bonded joints
ESDU	Engineering Science Data Unit, UK	Software for use in structural design	

carried out stress analyses using a variety of other methods, such as those based on Hashin's variational analysis using the principle of minimum complementary energy [2]. Reviews of these closed-form theories and their assumptions can be found in [3–6]. As the analytical equations become more complex (including factors such as stress variation through the adhesive thickness, plasticity, thermal effects, etc.), there is a greater requirement to use computing power to solve for the stresses. Hart-Smith [7] had a great influence on the methods used for stress analysis of adhesive joints. Versions of this method have been prepared as Fortran® programs and have been used extensively in the aerospace industry. Other analyses have been implemented in spreadsheets or as a program for personal computers (PCs). Although simplified analytical procedures for designing adhesively bonded joints are available in the form of PC-compatible software [8], these packages are limited in number and scope. As with all design tools, the effectiveness of the analysis is directly related to the user's knowledge and, therefore, it is advisable that the user has a good understanding of engineering design and material behavior. The software packages are there to assist in the design of efficient joints. A brief overview of commercial PC-based analysis/design software packages is given in Table 1 [9]. The main features of each software package are identified. As it is shown in Table 1, the existing software packages are very specific and most of them cover only one or two joints geometries. Not all software packages can work with isotropic and anisotropic adherends, or include adhesive and adherend plasticity. Therefore, the creation of new software that gives the possibility of working with a set of different joint geometries, with composite adherends, adhesive and adherend plasticity and thermal effects would be very useful for the design engineer. To satisfy that need, software was created taking into account the aspects mentioned above, to better assist the design engineers in designing adhesive joints. The models implemented in the software were validated with experimental tests.

2. SOFTWARE DESCRIPTION

The objective was to supply design engineers with a toolbox of methods for a better and easier analysis of adhesive joints. In a first stage, a simple and intuitive web-interface was developed with a toolbox of methods and mathematical models, as shown schematically in Fig. 1. The website was designed for multiple purposes: user input of joint problems data, automatic model selection (based on the problem data available), graphical plot visualization of stress distribution, and calculation of failure load and database access management. The user

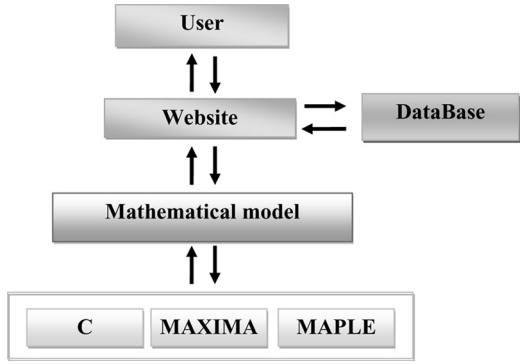

FIGURE 1 General description of the web-based software developed.

submits a set of data and then selects a model that "fits" the data of the problem. Once the mathematical model calculations are finished, the results achieved are presented to the user in the form of a graphical interface. The user can see a plot of the model results (for example, the shear stress over the overlap). The datasheet version of the results is also available if the user wants to process the results in a different way. The models used in the web software were implemented as computer programs following a simple set of rules: the programs of the models are connected to the server (it may or may not be on the same machine), the programs of the models work using a black-box implementation (only the input and output formats are known), and the programs of the models all use a normalized input/output set of rules. This design set allows pre-made programs, which follow the implementation format, to be incorporated in the project with minimum effort and retaining functionality. The program was developed in modules, so as to fulfill better the requirements described above. A modular system is composed of separate components that can be connected together. In modular architecture you can replace or add any one component (module) without affecting the rest of the system. The following modular architecture was used:

- Website module: All user-interface is conducted thought the web site. Therefore, usability was considered to be a major factor during development. The website was implemented using html managed with the help of the smarty template engine [10];
- Control module: The control module is comprised of a series of php [11] programs which process user input in order to correctly operate the mathematical models and visualize their output;

- Mathematical modules: Several mathematical models were implemented, each one representing its own module. The models used so far were implemented in the C programming language.

The software has five different mathematical models implemented (Volkersen [1], Goland and Reissner [12], Hart-Smith [7], Bigwood and Crocombe [13], and Adams *et al.* [14]). These models are described in detail in Section 3. The user can select the different models in the main page. After the model selection, the user can enter the necessary parameters for the selected model. When the user finishes entering the data, he/she can order the software to determine the stress distribution along the overlap joint and save the data in graphical or table format. The site is accessible at the website http://ni.fe.up.pt/~rteixeira/rjoints.

The previous web-based software was further developed in the form of executable application software programmed in Matlab (MathWorks, Natick, Massachusetts, USA). This software was created to be more intuitive and user-friendly, and being a local program makes the software more robust and secure. "Joint Designer" was the name selected for the software created in Matlab. The software organization is described in Fig. 2. Each of the steps presented in Fig. 2 is described in detail next.

2.1. Selection of Joint Type and Loading

The joints that have been implemented are the single lap joint (SLJ), the double lap joint (DLJ), and the sandwich joint (see Fig. 3). Once the user selects the type of joint, a new window appears for the user to select the type of load applied to the joint. The software allows the definition of the boundary loads in the sandwich joint, permitting the analysis of various configurations of adhesive joints under complex loading, consisting of tensile and shearing forces and a bending moment at the ends of the adherends. A simulation of almost any type of geometry can be done once the loads can be simplified to this form. The thermal effects are considered only for the DLJ. The tubular joint is not available at the moment but will also be implemented in the future.

2.2. Selection of Material Behavior

The user has the possibility of choosing the type of material behavior for both adhesive and adherends. The user can select between elastic or plastic and between isotropic or anisotropic (see Fig. 4 for the case of a single lap joint). Only the adherends can have anisotropic properties.

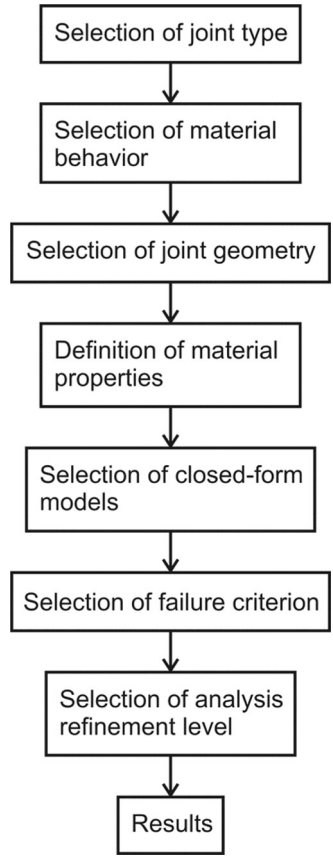

FIGURE 2 Matlab software general description.

Anisotropic properties only cover laminate layer composites (see Section 6).

2.3. Joint Geometry and Loading

The joint geometry data consists in the thickness of the adherends and adhesive layer, the overlap length, and joint width. The magnitude of the load is also introduced here.

2.4. Material Properties

In the material properties window, the user has to introduce the Young's modulus and the Poisson's ratio of both adherends and adhesive (see Fig. 5 for the SLJ).

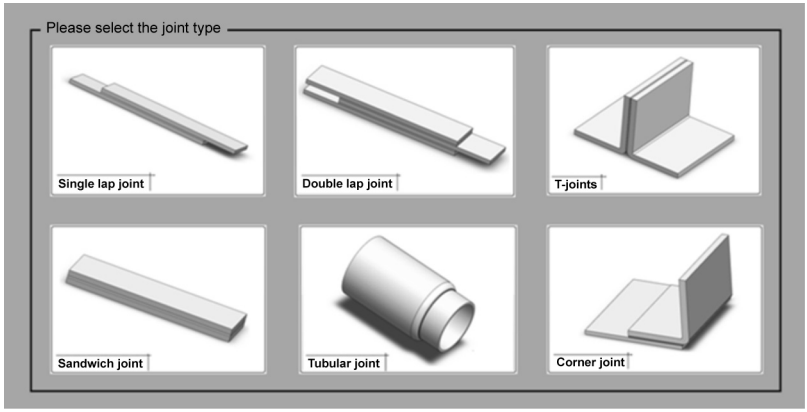

FIGURE 3 Joint type selection window.

If the adherend is a laminate composite, the user has to introduce the Young's modulus and the Poisson's ratio in the longitudinal and transverse direction. Then, the user has to insert the number of laminate layers and the orientation of the fibers in each laminate layer in a vector format (see Fig. 6).

If the adhesive is plastic, the yield strength and failure strain need to be introduced.

2.5. Closed-Form Models

The user then chooses the available models to determine the stress distribution (see Fig. 7). The software only shows to the user the

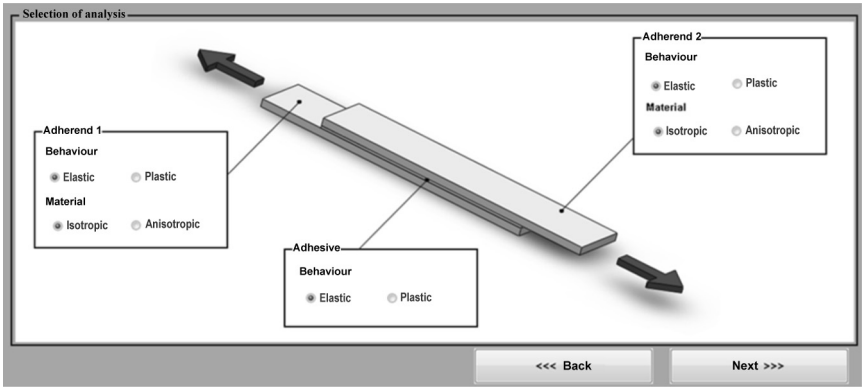

FIGURE 4 Selection of material behavior for the SLJ.

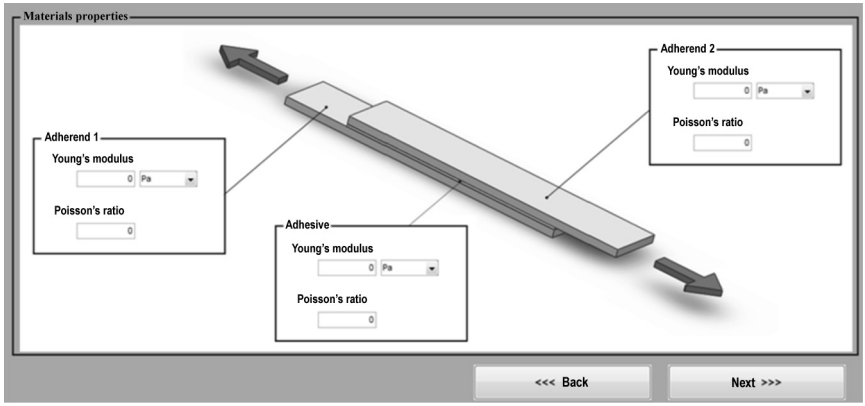

FIGURE 5 Material properties definition window for the SLJ.

models that can be run for the selected material behavior and geometry. For example, if the user previously selected to include the plasticity of the adherend, the only model available is that of Adams *et al.* [14]. A description of the closed-form models implemented in the software is presented in Section 3.

2.6. Selection of Failure Criterion

After the selection of the closed-form model, the user can select a failure criterion. The software has a total of four criteria: the shear

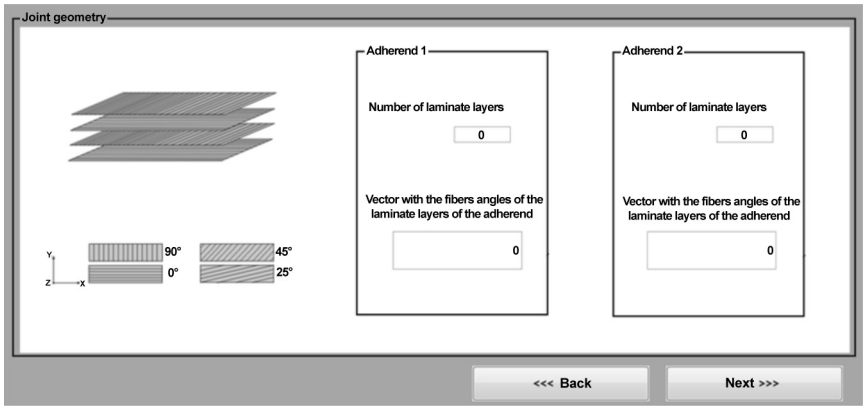

FIGURE 6 Characterization of the adherend layers window in the case of composite laminates.

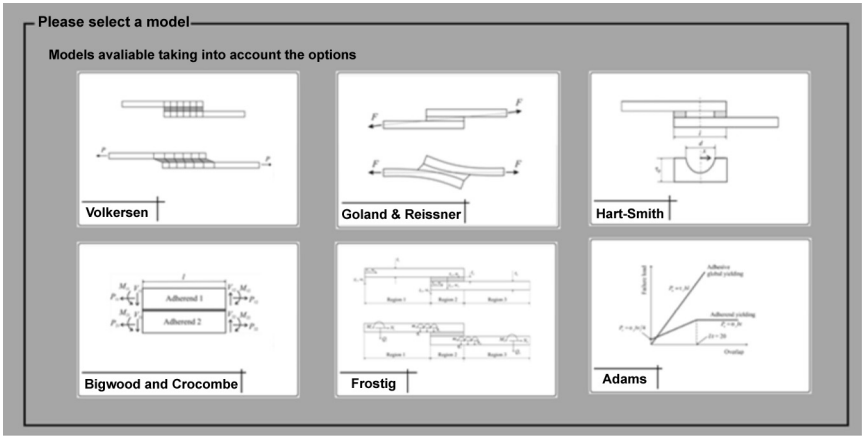

FIGURE 7 Analytical models selection window.

stress, the peel stress, the von Mises stress limit (all in the adhesive), and the adherend yield stress (see Fig. 8). According to the model selected, the software makes available or unavailable the selection for the criterion. For example, the von Mises stress limit is only available for the Bigwood and Crocombe model. In the case of the Hart-Smith model [15], the criterion is automatically defined when the model is selected and corresponds to the adhesive shear failure strain. It should be borne in mind that all adhesive stresses given by models based on beam or plate theories refer to what occurs on the adhesive mid plane, whilst failure initiates close to the adhesive/adherend interface. Therefore, one could argue that the calculated

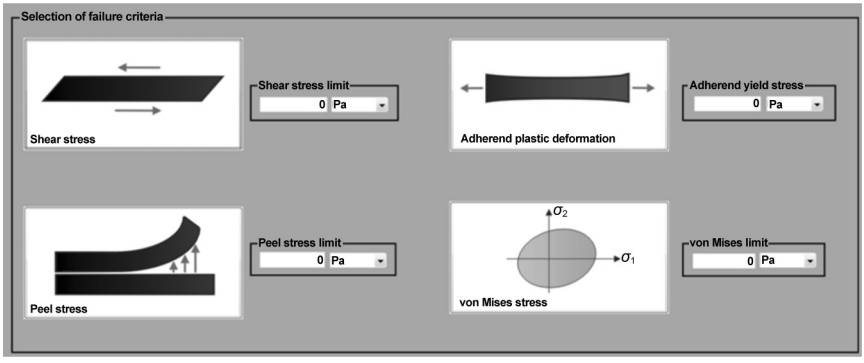

FIGURE 8 Failure criteria selection window.

stress values are not those which "break" the adhesive. However, because the models that give the interface stresses are generally too conservative due to the singularities at the adhesive/adherend interface, the mid-plane stresses are generally more realistic [6].

2.7. Selection of Analysis Refinement Level

In this window (see Fig. 9) the user can choose the level of analysis refinement, done by selecting the number of calculation points along the overlap length. The software permits three levels of analysis. The rough analysis calculates 50 points equally distributed along the overlap, the normal analysis calculates 200 points, and the refined analysis calculates 500 points. The user has also the possibility to choose the number of calculation points by selecting the custom analysis button and entering the number of points.

2.8. Results

Finally, the results are shown to the user. The results window shows the data in two ways. A table window allows the user to look at particular points along the overlap, while the plot form allows the user to have a global view of the stress distributions (see Fig. 10 for the case of the Goland and Reissner's analysis [12]). If the user selects the labelled "Save data (txt)" button, a small window appears where the user can type the path and name of the text file. If the user selects the "Print shear" or "Print peel" labelled buttons, a pdf file is created in the computer, with the name that the user chooses in a small print window that appears just after the user selects the print buttons.

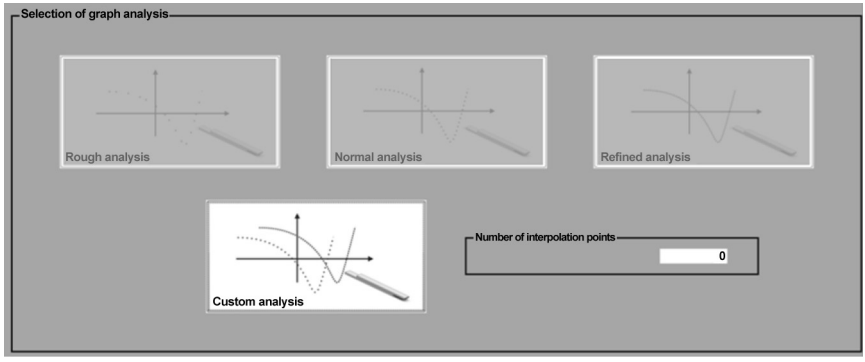

FIGURE 9 Selection of the analysis refinement level.

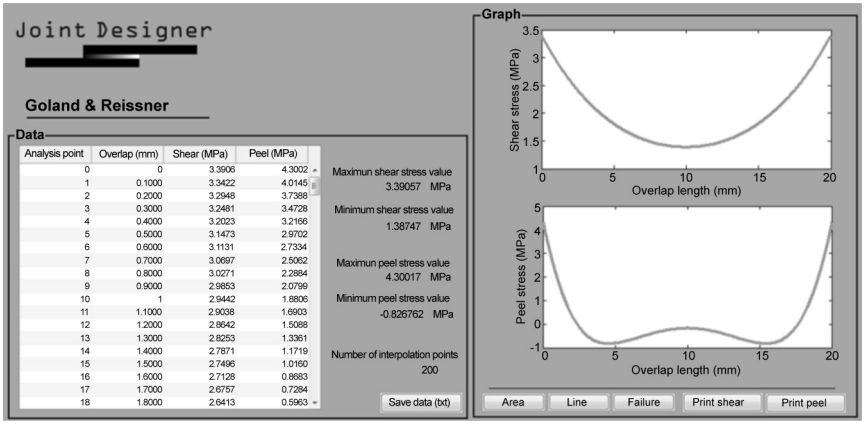

FIGURE 10 Results window in the case of Goland and Reissner's analysis [12].

If the user has previously selected a failure criterion and entered the maximum limit for the failure criterion, a red line appears in the plots indicating the limit of stress failure. If the stress distribution passes this value, the limit stress line appears in red.

3. ANALYTICAL MODELS IMPLEMENTED IN THE SOFTWARE

3.1. Volkersen

Volkersen [1] introduced the concept of differential shear. It was assumed that the adhesive deforms only in shear and that the adherends can deform in tension. The reduction of the strain in the adherends along the overlap and the continuity of the adhesive/adherend interface cause a non-uniform shear strain (and stress) distribution in the adhesive layer. The shear stress is maximum at the ends of the overlap and is much lower at the middle, as shown in Fig. 11. However, this analysis does not account for the bending effect caused by the eccentric load path of SLJs. The solution is more representative of DLJ than a SLJ since in a DLJ the overall bending of the adherends is not as significant as in the SLJ. The adhesive shear stress distribution (τ) is given by:

$$\tau = \frac{P}{bl}\frac{w}{2}\frac{\cos \mathrm{h}(wX)}{\sin \mathrm{h}(w/2)} + \left(\frac{\psi - 1}{\psi + 1}\right)\frac{w}{2}\frac{\sin \mathrm{h}(wX)}{\cos \mathrm{h}(w/2)}, \quad (1)$$

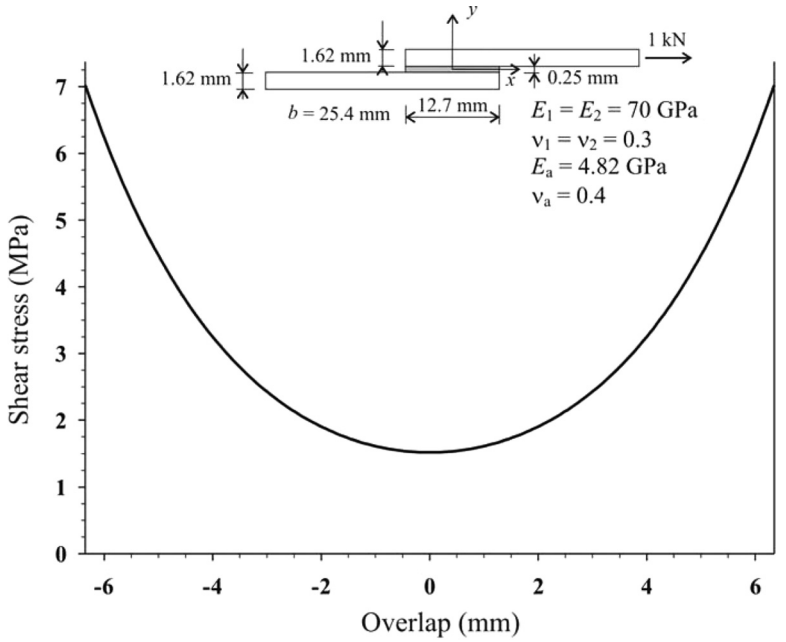

FIGURE 11 Volkersen's adhesive shear stress distribution [5] for aluminium alloy adherends and an epoxy adhesive.

where P is the applied load, b the joint width, l the overlap,

$$w^2 = (1+\psi)\phi$$
$$\psi = t_t/t_b$$
$$\phi = \frac{G_a l^2}{E t_t t_a}$$
$$X = x/l \quad -\frac{1}{2} \le X \le \frac{1}{2}$$

t_t the top adherend thickness, t_b the bottom adherend thickness, E the adherend modulus, G_a the adhesive shear modulus, and t_a the adhesive thickness. The origin of the longitudinal coordinate, x, is the middle of the overlap.

3.2. Goland and Reissner

The load in the SLJ is not co-linear and this gives rise to a bending moment. Because of this bending moment, the joint will rotate, altering the direction of the load line with the tendency of the applied

tensile forces to come into line. As the joint rotates, the bending moment will decrease, giving rise to a nonlinear geometric problem where the effects of the large deflections of the adherends must be accounted for. In addition to the shear stress, peel stress is also present, as shown in Fig. 12. The first to consider these effects were Goland and Reissner [12]. Algebraic solutions for the elastic shear and peel adhesive stresses are available. The expression for the adhesive shear stress is:

$$\tau = -\frac{1}{8}\frac{\overline{P}}{c}\left\{\frac{\beta c}{t}(1+3k)\frac{\cosh\left(\frac{\beta c}{t}\frac{x}{c}\right)}{\sinh\left(\frac{\beta c}{t}\right)} + 3(1-k)\right\}, \tag{2}$$

where $\overline{P}$ is the applied tensile load per unit width, c half of the overlap length, and t the adherend thickness,

$$\beta^2 = 8\frac{G_a}{E}\frac{t}{t_a}$$

$$k = \frac{\cosh(u_2 c)}{\cosh(u_2 c) + 2\sqrt{2}\sinh(u_2 c)}$$

$$u_2 = \sqrt{\frac{3(1-\nu^2)}{2}}\frac{1}{t}\sqrt{\frac{\overline{P}}{tE}}.$$

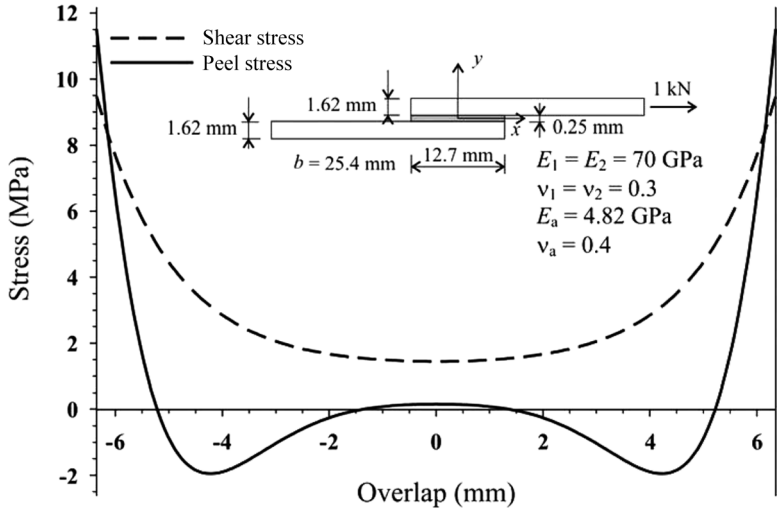

FIGURE 12 Goland and Reissner's adhesive shear and peel stress distributions [12] for aluminium alloy adherends and an epoxy adhesive.

The expression for the adhesive peel stress is:

$$\sigma = \frac{1}{\Delta}\frac{\overline{P}t}{c^2}\left[\left(R_2\lambda^2\frac{k}{2} + \lambda k'\cos\mathrm{h}(\lambda)\cos(\lambda)\right)\cosh\left(\frac{\lambda x}{c}\right)\cos\left(\frac{\lambda x}{c}\right) + \left(R_1\lambda^2\frac{k}{2} + \lambda k'\sin\mathrm{h}(\lambda)\sin(\lambda)\right)\sinh\left(\frac{\lambda x}{c}\right)\sin\left(\frac{\lambda x}{c}\right)\right], \quad (3)$$

where

$$\lambda = \gamma\frac{c}{t}$$

$$\gamma^4 = 6\frac{E_\mathrm{a}}{E}\frac{t}{t_\mathrm{a}}$$

E_a is the adhesive Young's modulus

$$k' = \frac{kc}{t}\sqrt{3(1-\nu^2)\frac{\overline{P}}{tE}}$$

$$R_1 = \cos\mathrm{h}(\lambda)\sin(\lambda) + \sin\mathrm{h}(\lambda)\cos(\lambda)$$

$$R_2 = \sin\mathrm{h}(\lambda)\cos(\lambda) - \cos\mathrm{h}(\lambda)\sin(\lambda)$$

$$\Delta = \frac{1}{2}(\sin(2\lambda) + \sin\mathrm{h}(2\lambda)).$$

The origin of the longitudinal coordinate, x, is the middle of the overlap.

3.3. Hart-Smith

One of the most important works considering adhesive plasticity was done by Hart-Smith for SLJs [15]. Hart-Smith's solutions accounted for adhesive plasticity, using an elastic-plastic shear stress model. He also included adherend stiffness imbalance and thermal mismatch. If we allow for adhesive plasticity, the joint strength prediction is higher than for an elastic analysis because a larger failure strain is used. The maximum lap joint strength was calculated by using the maximum shear strain as the failure criterion. Any differences between the adherends result in a decrease of the joint strength.

To characterize the adhesive behavior, Hart-Smith chose an elasto-plastic model (see Fig. 13) such that the ultimate shear stress and strain in the model are equal to the ultimate shear stress and strain of the real stress-strain curve of the adhesive, the two curves having the same strain energy. The maximum lap joint strength was calculated by using the maximum shear strain as the failure criterion, as shown in Fig. 13.

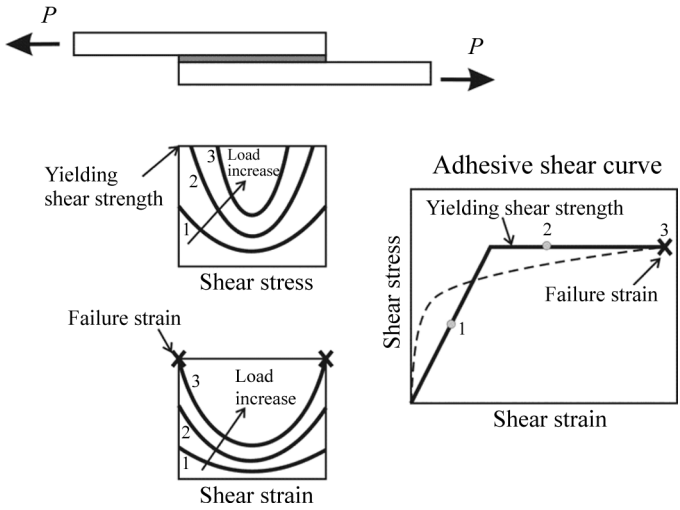

FIGURE 13 Schematic explanation of shear plastic deformation of the adhesive according to Hart-Smith [15].

Hart-Smith [15] gives a closed-form algebraic solution for the elastic shear and peel adhesive stresses. The origin of x is the middle of the overlap. The adhesive shear stress is given by

$$\tau = A_2 \cos \mathrm{h}(2\lambda' x) + C_2, \tag{4}$$

where

$$\lambda' = \sqrt{\left[\frac{1+3(1-\nu^2)}{4}\right]\frac{2G_\mathrm{a}}{t_\mathrm{a}Et}}$$

$$A_2 = \frac{G_\mathrm{a}}{t_\mathrm{a}Et}\left[\overline{P} + \frac{6(1-\nu^2)M}{t}\right]\frac{1}{2\lambda' \sin \mathrm{h}(2\lambda' c)}$$

$$C_2 = \frac{1}{2c}\left[\overline{P} - 2\frac{A_2}{2\lambda'}\sin \mathrm{h}(2\lambda' c)\right]$$

$$M = \overline{P}\left(\frac{t+t_\mathrm{a}}{2}\right)\frac{1}{1+\xi c + \frac{\xi^2 c^2}{6}}$$

$$\xi^2 = \frac{\overline{P}}{D}$$

$$D = \frac{Et^3}{12(1-\nu^2)}.$$

The adhesive peel stress is given by

$$\sigma = A\cos\mathrm{h}(\chi x)\cos(\chi x) + B\sin\mathrm{h}(\chi x)\sin(\chi x), \tag{5}$$

where

$$\chi^4 = \frac{E_\mathrm{a}}{2Dt_\mathrm{a}}$$

$$A = -\frac{E_\mathrm{a}M[\sin(\chi c) - \cos(\chi c)]}{t_\mathrm{a}D\chi^2 e^{(\chi c)}}$$

$$B = \frac{E_\mathrm{a}M[\sin(\chi c) + \cos(\chi c)]}{t_\mathrm{a}D\chi^2 e^{(\chi c)}}.$$

Hart-Smith also considered adhesive shear stress plasticity, keeping the peel stress elastic. The shear stress is modelled using a bi-linear elastic-perfectly plastic approximation. The overlap is divided into three regions, a central elastic region of length d and two outer plastic regions. The overlap length is l and, for a balanced lap-joint, both non-linear regions have length $(l-d)/2$. Coordinates x and x' are defined in these regions, as shown in Fig. 14. The problem is solved in the elastic

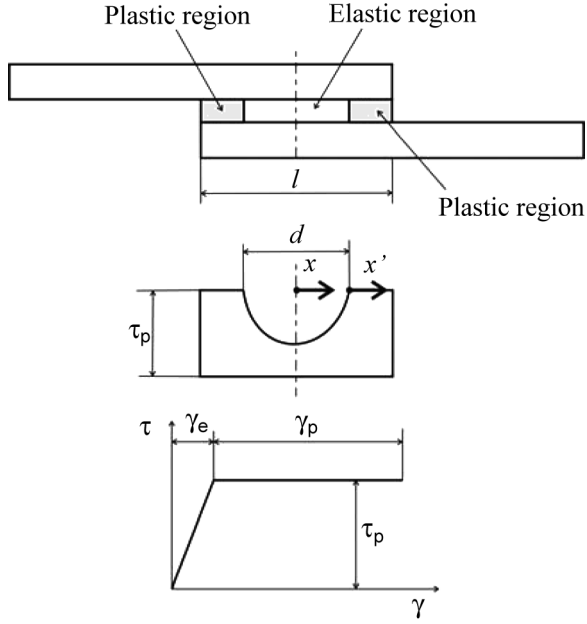

FIGURE 14 Plasticity in the adhesive according to Hart-Smith [15].

region in terms of the shear stress according to

$$\tau = A_2 \cos h(2\lambda' x) + \tau_p(1 - K) \tag{6}$$

and the shear strain in the plastic region according to

$$\gamma = \gamma_e\{1 + 2K[(\lambda' x')^2 + \lambda' x' \tan h(\lambda' d)]\}, \tag{7}$$

where τ_p is the plastic adhesive shear stress and

$$A_2 = \frac{K\tau_p}{\cos h(\lambda' d)}.$$

K and d are solved by an iterative approach using the following equations:

$$\frac{\overline{P}}{l\tau_p}(\lambda' l) = 2\lambda'\left(\frac{l-d}{2}\right) + (1-K)(\lambda' d) + K\tan h(\lambda' d) \tag{8}$$

$$\left[1 + 3k(1-\nu^2)\left(1 + \frac{t_a}{t}\right)\right]\frac{\overline{P}}{\tau_p}\lambda^2\left(\frac{l-d}{2}\right) = 2\left(\frac{\gamma_p}{\gamma_e}\right) + K\left[2\lambda'\left(\frac{l-d}{2}\right)\right]^2 \tag{9}$$

$$2\left(\frac{\gamma_p}{\gamma_e}\right) = K\left\{\left[2\lambda'\left(\frac{l-d}{2}\right) + \tan h(\lambda' d)\right]^2 - \tan h^2(\lambda' d)\right\}, \tag{10}$$

where γ_e is the elastic adhesive shear strain and γ_p the plastic adhesive shear strain (see Fig. 14). An initial value of the bending moment factor, k, is given and the system solved for P, K, and d. This process is repeated until there is convergence of k.

3.4. Bigwood and Crocombe

Bigwood and Crocombe [13] initially proposed a closed-form elastic analysis of a sandwich specimen subjected to general loading (see Fig. 15). The origin of x is the left end of the overlap. A general elastic

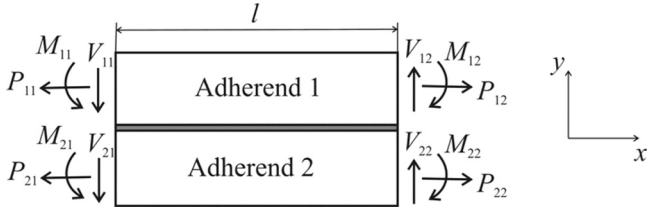

FIGURE 15 Bigwood and Crocombe's diagram of adherend-adhesive sandwich under general loading [13].

analysis and a simplified peel and shear analysis was done. In the simplified analysis, two-parameter design formulae that accurately determined the adhesive shear and peel stress peaks at the ends of the overlap were proposed. For similar adherends, the results yield exact values in relationship to the general analyses but there are limitations for dissimilar adherends. In any case, the formulae provide a simple initial estimate of joint strength. To facilitate the analysis to produce design formulae for determining the peak peel and shear stresses, the adhesive stresses (peel and shear) were uncoupled. The simplified adhesive peel stress is given by

$$\sigma = A_1 \cos(K_5 x)\cos \mathrm{h}(K_5 x) + A_2 \cos(K_5 x)\sin \mathrm{h}(K_5 x) + A_3 \sin(K_5 x)\cos \mathrm{h}(K_5 x) + A_4 \sin(K_5 x)\sin \mathrm{h}(K_5 x) \quad (11)$$

and the simplified adhesive shear stress is given by

$$\tau = C_1 \cos \mathrm{h}(K_6 x) + C_2 \sin \mathrm{h}(K_6 x) + C_3. \quad (12)$$

The constants $A_{1\text{–}4}$, $K_{5\text{–}6}$, and $C_{1\text{–}3}$ can be found in Bigwood and Crocombe's paper [13].

Adhesive plasticity was introduced in a later paper [16]. The nonlinear adhesive joint problem consists of a system of six, first-order, nonlinear differential equations. These six differential equations, in conjunction with the adhesive yield model and a continuous mathematical model to represent the adhesive stress-strain curve, are solved numerically using a finite difference technique.

The adherend plasticity was included in a later paper [17]. The problem is still governed by a system of six first-order, nonlinear differential equations, but some functions appearing in that system are implicit and take different forms according to the type of loading which makes the problem more complex. The finite difference technique was also used to solve the problem.

The great advantage of the model of Bigwood and Crocombe is that it is a sandwich that can be used for any type of joint provided the boundary conditions are known. The present software includes the general elastic analysis. The adhesive plasticity is partially implemented. There are still some convergence problems in the boundary value problem of the Matlab solver. To run the model it is necessary to solve two sets of six nonlinear, first-order differential equations. The first set needs initial values to enable the resolution of the system, giving a start value to the second set of equations. In the second set, the stress distributions along the overlap length are given. But using the boundary value problem of the Matlab solver, the values of the second equations set do not converge. This problem should be solved shortly.

The adherend plasticity is not implemented because of the complexity of the mathematical resolution. For that case, the model of Adams *et al.* [14] is simpler to use.

3.5. Adams *et al.*

Adams *et al.* [14] proposed a simple predictive model that gives the adhesive global yielding and the adherend yielding. For substrates that yield, a plateau is reached for a certain value of overlap corresponding to the yielding of the adherend, the joint strength being easily predicted. For intermediate or brittle adhesives and non-yielding adherends, the analysis is less robust and the author suggests using the finite element method or a more complete analytical solution. The failure load of the adhesive joint (P_a), with elastic adherends, corresponds to the total plastic deformation of the adhesive (*i.e.*, everywhere in yield), and the maximum load that can be carried which just creates adherend yield corresponds to the failure load of the adhesive joint (P_s). The design methodology is represented graphically in Fig. 16 and described next. In a SLJ with elastic adherends, the load corresponding to the total plastic deformation of the adhesive (*i.e.*, everywhere in yield) is:

$$P_a = \tau_y bl, \tag{13}$$

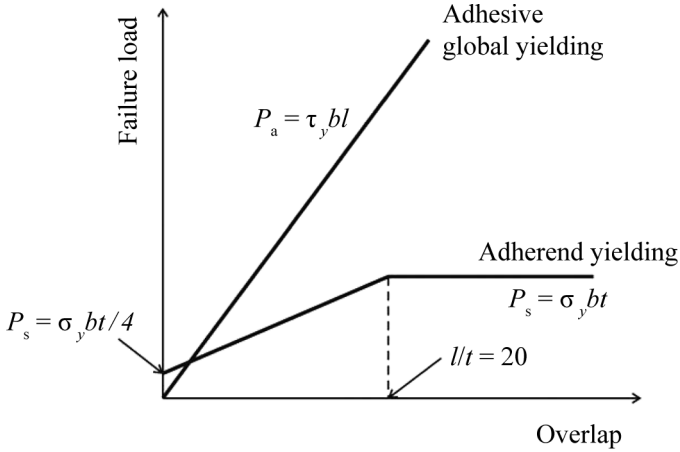

FIGURE 16 Simple design methodology of single lap joints based on the adherend yielding according to Adams *et al.* [14].

where P_a is the failure load of the adhesive joint and τ_y is the yield strength of the adhesive. The direct tensile stress (σ_t) acting in the adherend due to the applied load, P, is

$$\sigma_t = P/bt. \tag{14}$$

If there is bending (as per Goland and Reissner [12]), the stress at the inner adherend surface (σ_s) due to the bending moment, M, is

$$\sigma_s = 6M/bt^2, \tag{15}$$

where $M = kPt/2$ [12]. The variable k is the bending moment factor which reduces (from unity) as the lap rotates under load. The stress acting in the adherend is the sum of the direct stress and the bending stress. Thus, the maximum load which can be carried which just creates adherend yield (P_s) is:

$$P_s = \sigma_y bt/(1 + 3k), \tag{16}$$

where σ_y is the yield strength of the adherend. For low loads and short overlaps, k is approximately 1. Therefore, for such a case,

$$P_s = \sigma_y bt/4. \tag{17}$$

However, for joints which are long compared with the adherend thickness, such that $l/t \geq 20$, the value of k decreases and tends to zero. In this case, the whole of the cross-section yields in tension and

$$P_s = \sigma_y bt. \tag{18}$$

3.6. Frostig

The principle of virtual displacements, a variational principle, was used to derive the governing equations, the boundary conditions, and the continuity requirements [18]. The shear-stress-free condition at the ends of the overlap was modelled. The adhesive shear stress was considered constant through the adhesive thickness and the peel stress was allowed to vary through the thickness. The adherends were modelled as linearly-elastic, thin beams or panels (wide beams) obeying the Euler-Bernoulli assumptions. The adherends could be either metal or laminated composites. The shear and transverse normal (through thickness) deformations in the adherends were neglected. This model considers composite materials in its analysis, and gives the elastic shear and peel stress in the adhesive. The SLJ is divided into three regions, the left end side and right end side outer adherends

(Regions 1 and 3) and the overlap (Region 2). The governing equations and boundary conditions and the continuity requirements are derived for each region using the principle of virtual displacements:

$$\partial U + \partial V \equiv \partial W = 0, \tag{19}$$

where ∂U and ∂V are the internal and the external virtual work, and ∂W is the total virtual work. One of the main advantages of Frostig *et al.*'s model is the ability to partition the joint easily for the inclusion of more than one adhesive or variations in the adherend geometry. The rotation of the joint due to the eccentric load path that creates a nonlinear geometric problem was not included in Frostig's model. We have here modified Frostig's analysis by considering the transverse (thickness direction) adherend displacements in the bending moment expression outside the overlap region. The governing equations in Regions 1 and 3 have simple, closed-form solutions that can be obtained by simple integration. The Region 2 (overlap) governing equations consist of a system of seven linear differential equations with constant coefficients. The closed-form solution is more complex and is better solved by using a mathematical computer code. Due to its mathematical complexity, more than 300 command lines in the Matlab m file implementation are needed. The Frostig's model is mathematically implemented, but because of its complexity more time is needed to fully complete the Frostig's model to a user level.

3.7. Comparison Between Models

A summary of the implemented model is shown in Tables 2 and 3. Table 2 shows the different possibilities of analysis for each analytical model implemented in the software, showing the elasticity and/or plasticity of the materials, the geometries covered, and the results given. In Table 3, the failure criterion is shown for each model. For the models that have two criteria, the one that is first exceeded is the criterion followed for a given case. Table 4 indicates for each adhesive the shear strength (τ_r), the tensile strength (σ_r), the shear failure strain (γ_r), and the tensile failure strain (ε_r). The tensile properties were obtained from the tensile stress-strain curves presented in Fig. 17 and the shear properties were deduced from the tensile properties using the Dolev and Ishai yielding criterion [19] using a relation between the compressive and tensile strength of 1.3, a value typical for structural adhesives [20].

TABLE 2 Comparison Between the Models Implemented in the Software

Models	Adhesive elastic	Adhesive plastic	Adherend elastic	Adherend plastic	Isotropic adherends	Anisotropic adherends	Geometries covered	Results given
Volkersen	Yes	No	Yes	No	Yes	No	SLJ and DLJ	Shear stress
Goland and Reissner	Yes	No	Yes	No	Yes	No	SLJ	Shear and peel stresses
Hart-Smith	Yes	Yes	Yes	No	Yes	No	SLJ and DLJ	Shear and peel stresses
Bigwood and Crocombe	Yes	Yes	Yes	No	Yes	No	Sandwich	Shear, peel, and von Mises stresses
Adams *et al.*	Yes	Yes	Yes	Yes	Yes	No	SLJ and DLJ	Failure load
Frostig	Yes	No	Yes	Yes	Yes	Yes	SLJ	Shear and peel stresses

TABLE 3 Failure Criteria Used for the Models Implemented (τ shear stress, τ_r shear strength, σ peel stress, σ_r tensile strength, γ shear strain, γ_r shear failure strain, ε_{eq} equivalent strain (von Mises), ε_r tensile failure strain, and GY global yielding—all in the adhesive)

Models	Analysis	Failure criterion
Volkersen	Linear	$\tau > \tau_r$
Goland and Reissner	Linear	$\tau > \tau_r$ or $\sigma > \sigma_r$
Hart-Smith	Linear	$\tau > \tau_r$ or $\sigma > \sigma_r$
	Non-linear	$\gamma > \gamma_r$ or GY
Bigwood and Crocombe	Linear	$\tau > \tau_r$ or $\sigma > \sigma_r$
	Non-linear	$\varepsilon_{eq} > \varepsilon_r$ or GY
Frostig	Linear	$\tau > \tau_r$ or $\sigma > \sigma_r$
Adams	Elastic/plastic adherend and ductile adhesives	GY or Adherend yielding

TABLE 4 Adhesive Properties Used in the Failure Criteria (τ_r shear strength, σ_r tensile strength, and γ_r shear failure strain)

Adhesive	σ_r (MPa)	ε_r (%)	τ_r (MPa)	γ_r (%)
AV118	73	5.8	48	12.2
Araldite 420	38	8.3	25	16.4

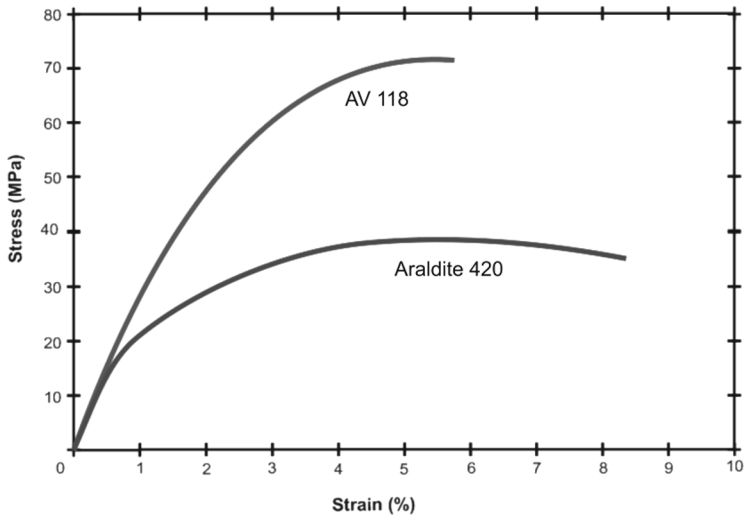

FIGURE 17 Stress-strain curves of Araldite 420 and AV 118 adhesives (1 mm/min displacement rate).

4. JOINT STRENGTH PREDICTION

The software developed would be of little use if the models implemented could not predict properly the failure load of practical joints. Therefore, experimental tests were carried out to validate the models implemented. The true test for a model is to predict joint strength for a variety of conditions.

4.1. Experimental Details

4.1.1. Materials

Two paste adhesives were selected, one very stiff and brittle epoxy (AV118) and one less stiff and more ductile epoxy (Araldite® 420). Both adhesives were from Huntsman (Salt Lake City, UT, USA). Uniaxial testing was done on bulk specimens and the stress-strain curves are represented in Fig. 17. The adherend was an aluminium alloy from the 6000 series. The yield strength is 300 MPa [21].

4.1.2. Geometry of Specimens

Single lap joints (SLJ) were fabricated with an overlap of 12.5 mm and a width of 25 mm (see geometry in Fig. 18). The adhesive thickness was 0.5 mm. Tab ends were bonded to the edges to decrease the bending moment caused by the tensile test, although in a SLJ geometry it is impossible to have a pure shear stress.

4.1.3. Manufacture of Specimens

The bonding area was initially degreased with acetone, abraded with a #180 SiC sandpaper, and again cleaned with acetone before the application of the adhesive.

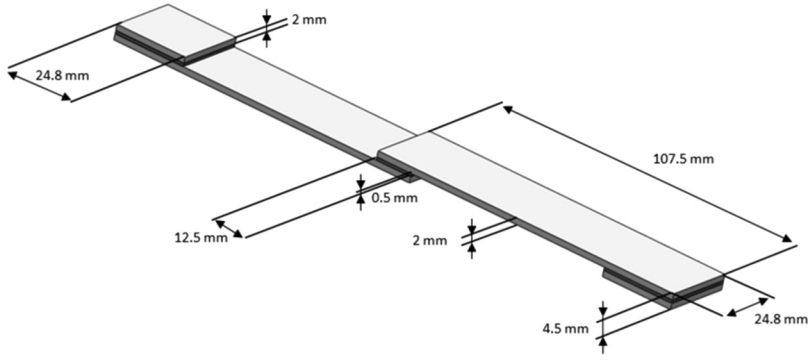

FIGURE 18 SLJ specimen geometry.

4.1.4. Test Procedure

The specimens were tested on a 200 kN Roell & Korthaus test frame (Zwick/Roell, Ulm, Germany). The test speed was 1 mm/min. At least three specimens were tested for each type of joint.

4.2. Results

The joints had an apparent adhesive failure with no visible adherend yielding. However, a scanning electron microscopy analysis and an X-ray photoelectron spectroscopy analysis showed that a thin layer of adhesive remained on the adherend surface (see Fig. 19). A similar scan of a clean interface was done. As expected, the analysis detected a large presence of aluminium. Others elements, like C and O, were detected but in a very small quantity when compared with aluminium.

Figure 20 shows the experimental results and the model predictions in terms of failure load for the AV 118 specimens. The models that best predict the experimental failure load are the linear models that consider the adhesive and the adherends as elastic, except the Volkersen and the Frostig models. The Volkersen's model does not take into account the rotation of the SLJ, which increases the predicted failure load compared with the other elastic models. The error between the predictions and the experimental values are relatively large, mainly due to the fact that the elastic models consider that the failure load of the SLJ specimens increases with the adhesive thickness, which in practice is not true. The elastic models predict the failure load with more accuracy for joints that have a thin adhesive layer, approximately 0.1–0.3 mm, as shown by da Silva *et al.* [6]. These values are the most used in practice because they allow for greater joint strength. It can be concluded that with brittle adhesives, the SLJ specimens failure load can be predicted using the linear models, this prediction being more accurate for joints that have a thin adhesive layer.

Figure 21 shows the experimental results and the model predictions in terms of failure load for Araldite 420 specimens. In the Araldite 420 case, only the models that consider adhesive plasticity compare well with the experimental values. The plasticity of the adhesive causes a stress redistribution along the overlap using the less stressed parts of the overlap [6]. The joint strength, thus, increases in relation to an adhesive with no ductility, where only the ends of the overlap work. It can be concluded that with ductile adhesives, the SLJ specimens failure load can be predicted using the models that consider adhesive plasticity.

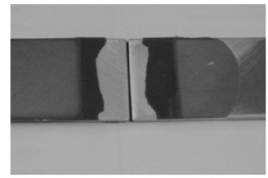

(a)

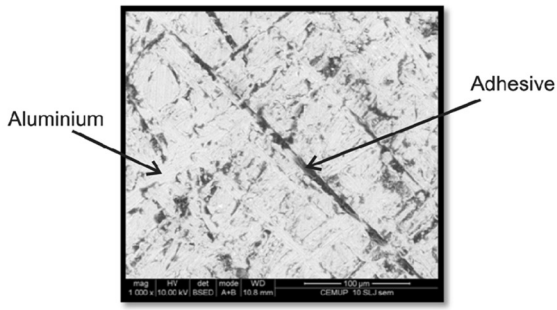

(b)

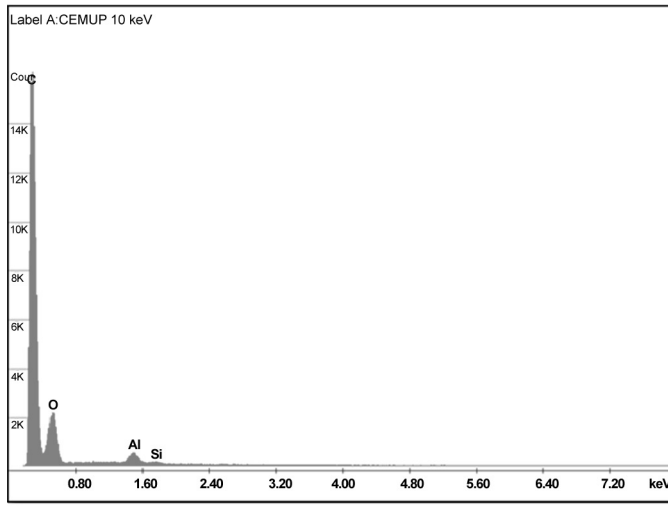

(c)

FIGURE 19 Surface analysis in the case of joints with Araldite 420: (a) macroscopic failed surfaces; (b) microscopic failed area; and (c) XPS analysis of the apparently adhesive failure showing the presence of carbon.

When the adherends yield, the only implemented model capable of predicting the failure load is that of Adams *et al.* Comparison with experimental values from [6] shows that the Adams'

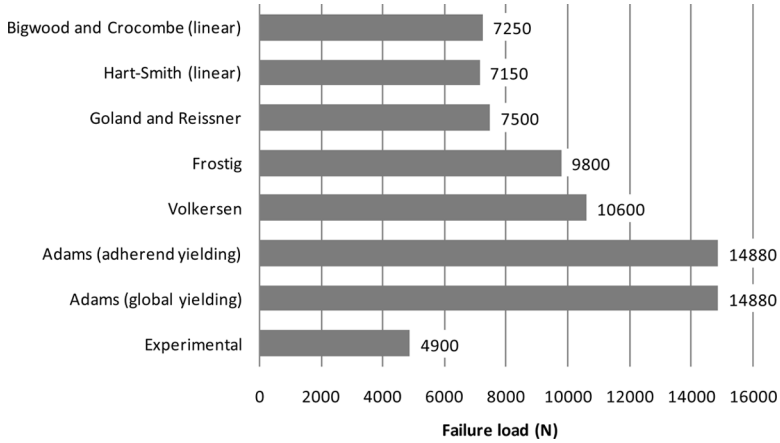

FIGURE 20 Comparison between the experimental data and the model predictions for AV118 specimens.

model for adherend plasticity predicts well the failure loads (see Fig. 22).

The validation of the models implemented in the software was carried out for one joint type and, therefore, unique values for overlap, adhesive thickness, substrate thickness, and substrate material. However, the same models were validated for other cases in [6], varying material and geometric parameters, and it was concluded that the models presented here are sufficient to cover the majority of the cases.

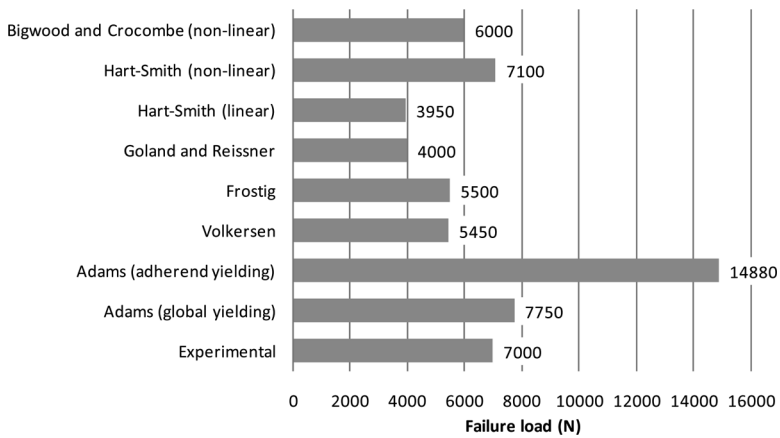

FIGURE 21 Comparison between the experimental data and the model predictions for Araldite 420 specimens.

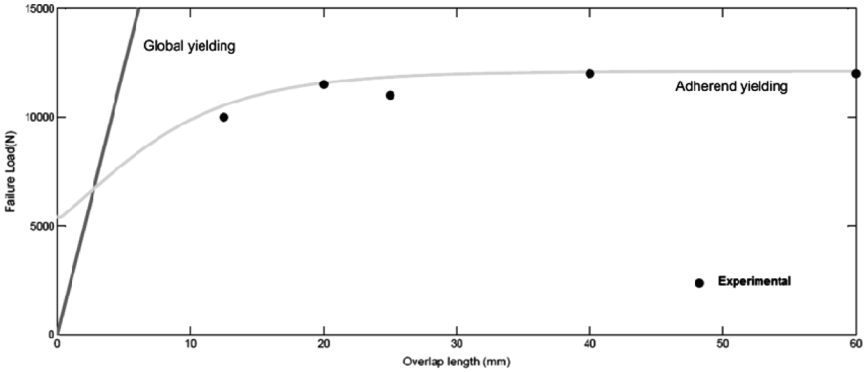

FIGURE 22 Comparison between the literature experimental values [6] and the Adams *et al.*'s model prediction.

5. CONCLUSIONS

User friendly software was developed to design in a simple way adhesive joints used in practice. The following conclusions can be drawn.

1. Six models of increasing complexity were implemented in the software to cover any situation that can occur in practice: elastic analysis, adhesive non-linear analysis, and adherend non-linear analysis. Isotropic and composite laminates can be simulated.
2. Lap joints and more complex joints can be analysed. The model of Bigwood and Crocombe [13] can simulate any type of joint that can be reduced to a sandwich joint.
3. The software consists of a step-wise process where the user goes through the following stages: selection of the joint type, selection of the material behavior, definition of joint geometry, definition of material properties, selection of the closed-form model, selection of the failure criterion, and selection of the analysis refinement. The results are presented graphically and in tabular form, and are easily exportable.
4. The joint strength prediction shows that the models implemented are sufficient for most of the practical case scenarios. However, the case of joints with composites still needs some work in the implementation.

ACKNOWLEDGMENTS

The authors thank the University of Porto (Project IPG96/2007) and the European Union (Projects Cordis FP6 31321 and METRI-2) for

supporting part of the work presented here. The experimental SLJ tests were performed at IFREMER (Brest, France) with the help of Dr. Peter Davies from IFREMER and Prof. Jean Yves Cognard from ENSIETA (Brest, France).

REFERENCES

[1] Volkersen, O., *Luftfartfoeshing* **15**, 41–47 (1938).
[2] Chalkley, P. and Rose, F., *International Journal of Adhesion and Adhesives* **21**, 241–247 (2001).
[3] Crocombe, A., Stress analysis, in *Adhesive Bonding: Science, Technology and Applications*, R. D. Adams (ed.), (Woodhead Publishing Limited, Cambridge, 2005).
[4] Banea, M. D. and da Silva, L. F. M., *Proceedings of the Institution of Mechanical Engineers, Part L, Journal of Materials: Design and Applications* **23**, 1–18 (2008).
[5] da Silva, L. F. M., das Neves, P. J. C., Adams, R. D., and Spelt, J. K., *International Journal of Adhesion and Adhesives* **29**, 319–330 (2009).
[6] da Silva, L. F. M., das Neves, P. J. C., Adams, R. D., Wang, A., and Spelt, J. K., *International Journal of Adhesion and Adhesives* **29**, 331–341 (2009).
[7] Hart-Smith, L. J., Adhesive-Bonded Double-Lap Joints NASA Contract Report, NASA CR-112235 (Hampton, Virginia, 1973).
[8] Oakeshott, J. L., Soininen, R., and Matthews, F. L., Review of composites—related software. Final report. Part I: Non-FE software, Technical Report TR96/01, (Centre for Composite Materials, Imperial College, London, 1996).
[9] National Physical Laboratory, *Design and Testing of Boued and Bolted Joints*, (Queen's Printer, Scotland, 2007).
[10] Smarty Template Engine, http://www.smarty.net/, last accessed February 1, 2009.
[11] PHP, http://www.php.net, last accessed February 1, 2009.
[12] Goland, M. and Reissner, E., *J. Appl. Mech.* **66**, A17–A27 (1944).
[13] Bigwood, D. A. and Crocombe, A. D., *International Journal of Adhesion and Adhesives* **9**, 229–242 (1989).
[14] Adams, R. D., Comyn, J., and Wake, W. C., *Structural Adhesive Joints in Engineering*, 2nd ed, (Chapman & Hall, London, 1997), pp. 122–127.
[15] Hart-Smith, L. J., Adhesive-Bonded Single-Lap Joints NASA Contract Report, NASA CR-112236 (Hampton, Virginia, 1973).
[16] Bigwood, D. A. and Crocombe, A. D., *International Journal of Adhesion and Adhesives* **10**, 31–41 (1990).
[17] Crocombe, A. D. and Bigwood, D. A., *Journal of Strain Analysis for Engineering Design* **27**, 211–218 (1992).
[18] Frostig, Y., Thomsen, O. T., and Mortensen, F., *Journal of Engineering Mechanics* **125**, 1298–1307 (1999).
[19] Dolev, G. and Ishai, O., *J Adhesion* **12**, 283–294 (1981).
[20] da Silva, L. F. M. and Adams, R. D., *Journal of Adhesion Science and Technology* **19** (2), 109–142 (2005).
[21] MatWeb Automation Creations, Inc., Blacksburg, Virginia, www.matweb.com, last accessed February 1, 2009.